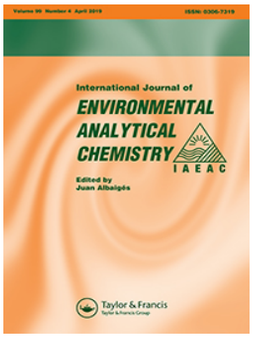

International Journal of Environmental Analytical Chemistry

ISSN: 0306-7319 (Print) 1029-0397 (Online) Journal homepage: https://www.tandfonline.com/loi/geac20

Photocatalytic degradation of organophosphate flame retardant TBEP: kinetics and identification of transformation products by orbitrap mass spectrometry

Panagiotis – Spyridon Konstas, Dimitra Hela, Aris Giannakas, Albanis Triantafyllos & Ioannis Konstantinou

To cite this article: Panagiotis – Spyridon Konstas, Dimitra Hela, Aris Giannakas, Albanis Triantafyllos & Ioannis Konstantinou (2019) Photocatalytic degradation of organophosphate flame retardant TBEP: kinetics and identification of transformation products by orbitrap mass spectrometry, International Journal of Environmental Analytical Chemistry, 99:4, 297-309, DOI: 10.1080/03067319.2019.1593399

To link to this article: https://doi.org/10.1080/03067319.2019.1593399

INTERNATIONAL JOURNAL OF ENVIRONMENTAL ANALYTICAL CHEMISTRY
2019, VOL. 99, NO. 4, 297–309
https://doi.org/10.1080/03067319.2019.1593399

Taylor & Francis
Taylor & Francis Group

ARTICLE

Photocatalytic degradation of organophosphate flame retardant TBEP: kinetics and identification of transformation products by orbitrap mass spectrometry

Panagiotis – Spyridon Konstas[a], Dimitra Hela[a], Aris Giannakas[b], Albanis Triantafyllos[a] and Ioannis Konstantinou[a]

[a]Department of Chemistry, University of Ioannina, Ioannina, Greece; [b]Department of Business Administration of Agricultural and Food Enterprises, University of Patras, Agrinio, Greece

ABSTRACT

The photocatalytic degradation of tris (2–butoxyethyl) phosphate (TBEP) flame retardant using visible light response catalysts TiO_2 /V_2O_5, (N,F-doped)-TiO_2/V_2O_5, and N-doped-$SrTiO_3$ has been studied by high-resolution orbitrap mass spectrometry. TBEP degradation followed first-order kinetics with half-life values ranging between 9.8 and 83.5 min. N-doped-$SrTiO_3$ was the catalyst with better photocatalytic performance while activity for TiO_2/V_2O_5 composites followed the trend: N, F- TiO_2/V_2O_5 > N-TiO_2/V_2O_5> TiO_2/V_2O_5. The identified degradation products (DPs) revealed hydroxylation, further oxidation and dealkylation as major degradation pathways. Based on the identified DPs and scavenging experiments, $^{\bullet}OH$ radical-mediated reactions can be considered for the degradation of TBEP using TiO_2 and $SrTiO_3$-based photocatalytic materials.

ARTICLE HISTORY
Received 16 November 2018
Accepted 5 March 2019

KEYWORDS
Organophosphates; flame retardants; TBEP; photocatalysis; oxidation pathways

1. Introduction

Heterogeneous photocatalysis is an efficient process for the removal of organic contaminants from surface waters and wastewaters. In addition, the use of photocatalysts with broader photoresponse is gaining importance in order to improve solar energy exploitation. So far, scientific work dealing with the removal of different classes of water pollutants like personal care products, pharmaceuticals, pesticides and other chemical additives such as plasticisers is accomplished with promising results [1,2]. In addition to these pollutants, flame retardants (FRs), i.e. chemical substances used for decreasing the risk of fire with wide applications in flammable products like electronics and plastics [3,4], represent an emerging and priority pollutant category because some compounds can exert toxic effects on human and environment [5,6]. FRs can be divided into four major classes depending on their chemical composition: inorganic, nitrogen – containing, phosphorus – containing and halogen-containing compounds [7]. Among them, the

CONTACT Ioannis Konstantinou iokonst@cc.uoi.gr

Ioannis Konstantinou: Paper presented at the 10th European Conference on Pesticides and Related Organic Micropollutants in the Environment & 16th Symposium on Chemistry and Fate of Modern Pesticides, Bologna (Italy), 12–14 September 2018

most commonly used group of flame retardants are the brominated flame retardants (BFRs) and organophosphate flame retardants (OPFRs) [8]. Through the years BFRs have either been restricted or the research upon them has been phased – out, so the production of alternative flame retardants like OPFRs has been increased [9–11]. Usually, OPFRs are mixed into the materials and they do not bond chemically. As a result, they are easily released into the environment during the production, use and disposal of products that contain them [8,12].

This study is focused on the tris(2–butoxyethyl) phosphate (TBEP) which belongs to the group of non – halogenated organophosphate ethers and is used as a flame retardant in plasticisers, lubricants, floor waxes and synthetic rubbers [13]. TBEP is considered to be plenty in effluent, surface, ground and drinking water (19.5–81.7 ng/L) [14] samples due to its water solubility (1.2 g/L) and low removal wastewaters treated with conventional methods [3,13,15–17]. According to a European Union-wide monitoring survey of wastewater treatment plant effluents, concentrations in water samples ranged from a few ng/L to a maximum of 43 μg/L [16].

Although a lot of research has been made in the field of heterogeneous photocatalysis during the previous years for the removal of BFRs [18–22], applications on the removal of OPFRs from surface waters and wastewaters has not been studied extensively. For example, only tris(2-chloroethyl) phosphate (TCEP), and tris(2-chloropropyl) phosphate (TCPP) photocatalytic degradation was studied using P25 and N,S-doped TiO_2 catalysts [23–26].

As a result, the aims of the present work are: (a) the application of heterogeneous photocatalysis using visible-light response catalysts such as V_2O_5/TiO_2, and N–doped $SrTiO_3$ under simulated solar light in order to remove TBEP pollutant from water matrices, a field that has not been studied so far; (c) The identification of the transformation products with the use of ultra-pressure liquid chromatography coupled to high resolution and accurate linear ion trap-orbitrap mass spectrometry (UPLC – LIT–Orbitrap-MS).

2. Experimental

2.1. *Chemicals*

TBEP (94%) was purchased by Sigma – Aldrich. Methanol (MeOH) and water of LC-MS grade was supplied by Fisher Scientific (Loughborough, UK) while isopropanol was supplied by Labscan (Dublin, Ireland). Milli Q water was obtained by an EVOQUA instrument (Polisher MFIIID Modul Ultra Clear ^{TM}). For removing photocatalyst particles from the solution samples, HVLP 0.45 μm filters by Millipore (Bedford, USA) was used. Oasis HLB (divinylbenzene/N-vinylpyrrolidone copolymer) cartridges (60 mg, 3 mL) from Waters (Milford, MA, USA) were used for the extraction of TPs.

2.2. *Photocatalytic materials*

TiO_2/V_2O_5 (TV), N,F-doped TiO_2/V_2O_5 (NTV, NFTV) with 5% wt loading of V_2O_5 calcined at two different temperatures, 450°C and 550°C, were used. The synthesis method (sol-gel impregnation) and characterisation of the materials were reported elsewhere [27]. Briefly, the characteristics of the materials are: 8.6–29.8 nm crystal size for TV450 and

NFTV550, respectively; specific surface area 28.5–80.2 m^2/g for NFTV550 and TV450, respectively; mesoporous structure, bang gap E_g = 2.54–2.79 eV for TV550 and TV450, respectively, hydrodynamic size in water 0.274–0.339 µm for NFTV450 and NFTV550, respectively.

N-doped $SrTiO_3$ (NSTO) catalysts have been used for the photocatalytic experiments. N-doped $SrTiO_3$ catalyst (GNSTO3; with a molar ratio of N:Sr: Ti 3:1:1) using glycine as dopant-source was also used. The synthesis of GNSTO3 catalysts is extensively described in the previous publication [28]. Briefly, 5 mL of aqueous solution containing an appropriate amount of glycine and 10 mmol $Sr(NO_3)_2$ were added dropwise into 40 mL of absolute ethanol containing 10 mmol of TBT and 2 mL glacial acetic acid under rigorous stirring, followed by evaporation to dryness at 50°C. The obtained dry gel was ground and calcined at 550°C/2 h with 10°C/min. Then, 100 ml of nitric acid 2M heated at 70°C was rinsed as a cleaning procedure, finally washed with distilled water until neutral pH values. The catalyst presented the following characteristics: $SrTiO_3$ cubic symmetry (78%)-$SrCO_3$ (22%), 14.2 nm crystal size, specific surface area 59.7 m^2/g, mesoporous structure (pore diameter 33.8 Å), bang gap E_g = 2.99, point of zero charge (PZC) pH = 5.52; hydrodynamic size in water 0.329 nm.

2.3. *Photocatalytic treatment*

Photocatalytic experiments were carried out in a solar simulator (Suntest XLS+) (2.2 kW xenon lamp, $\lambda > 290$ nm). Before illumination, suspensions of TBEP solutions containing 200 mg L^{-1} of photocatalyst were stirred at 600 rpm in the dark for 30 min to achieve adsorption equilibrium. The radiation intensity was kept constant at 500 W m^{-2} throughout the experiments. Samples (≈3 mL) were periodically withdrawn and filtered by 0.45 µm filters for further analysis. Photocatalytic experiments were run in triplicate. Relative errors lower than 5.2% were obtained in all cases.

2.4. *Analytical procedures*

The irradiated solution samples (3 mL) were extracted by means of solid-phase extraction (SPE), using Oasis HLB (divinylbenzene/N-vinylpyrrolidone copolymer) cartridges (60 mg, 3 mL) from Waters (Milford, MA, USA). SPE was performed using a 12-fold extraction box (Visiprep, Supelco, Bellefonte, PA, USA) fitted on a vacuum pump. The SPE cartridges were primarily conditioned with 3 mL of methanol, and 3 mL LC-grade water at a flow rate of 1 mL min^{-1}. Then, irradiated samples were added at a flow rate of 0.5 mL min^{-1}. Subsequently, the cartridges were dried by vacuum for 30 min followed by nitrogen stream for 5 min. The cartridges were eluted by using 2 × 2 mL of methanol as eluting solvent. Finally, the eluate was carefully evaporated to a final volume of 0.3 mL with a gentle stream of nitrogen, prior to analysis into the LC/MS instrument. An UPLC–ESI(+)-MS/MS system including an Accela LC pump and an LTQ-Orbitrap mass spectrometer (Thermo) was used for the characterisation of DPs of TBEP. The chromatographic analysis was run on a C18 Hypersil Gold, 100 mm x 2.1 mm i.d., 1.9 µm (Thermo) at 30 ◦C. Injection volume was 10 µL and flow rate 300 µL min^{-1}. Gradient mobile phase composition was adopted using water/5mM ammonium formate as solvent A and methanol/5mM ammonium formate as solvent B: 90/10 (1 min)

to 10/90 in 15 min, and 90/10 in 18 min (holding for 2 min). The following ESI-source parameters were adopted: sheath and auxiliary gas flow rate 38 and 8 (nitrogen, arbitrary units), respectively; source voltage at 3.40 kV; capillary voltage 40 V; tube lens 110 V; capillary temperature was maintained at 320◦C. For fragmentation study, 35% normalised collision energy and activation Q = 0.25 was used. Scan range was set between m/z 100–650 amu. The analysis was performed using a resolving power of 60,000 for MS and 30,000 for MS/MS. All data (chemical formulae, mass accuracy and ring-double bond (RDB) equivalent) were processed using also Xcalibur software. Mass accuracy of recorded ions was± 5 ppm.

3. Results and discussion

3.1. *Photocatalytic kinetics*

TBEP photocatalytic degradation kinetics using TV, NTV and NFTV catalysts is presented in Figure 1(a) while Figure 1(b) shows the linear transformation plots (natural logarithm of normalised concentration against irradiation time). Pseudo-first order kinetics were observed in all cases (R^2> >0.9560) with 0.0233 min^{-1} being the higher reaction constant determined for NFTV450. The photocatalytic activity for catalysts calcined at the same temperature (450°C or 550°C) followed the general trend: NFTV > NTV > TV. Catalysts calcined at a higher temperature (550°C) followed the same trend but slower kinetics compared with the corresponding catalysts calcined at 450°C. The above kinetics are consistent with the $^{\bullet}OH$ generation capability following also trend TV450< NTV450< NFTV450 according to a previous publication [27]. In addition, the photocatalytic degradation of TBEP using N-doped $SrTiO_3$ (G-NSTO3) catalyst is shown in Figure 2(a,b) for linearised form. This catalyst has also the ability to generate $^{\bullet}OH$ radicals being the principal oxidants during the photocatalytic process [28]. Table 1 summarises the photocatalytic kinetics parameters using different photocatalysts. In order to confirm the participation of $^{\bullet}OH$ radicals as the major oxidant species, scavenging experiments in the presence of isopropanol (10^{-2} M), a well-known $^{\bullet}OH$ quencher (1.9×10^9 M^{-1} s^{-1}), have been conducted for the best catalysts, NFTV450 and N-$SrTiO_3$. The apparent pseudo-first order reaction rate constants were 0.005 min^{-1} and 0.007 min^{-1} respectively, showing a strong retardation with approximately 80% and 90% reduction compared to the reaction rate constants in the absence of isopropanol.

For other advanced oxidation methods (UV/H_2O_2), tris(2-butoxyethyl) phosphate (TBEP) was shown to react fast with $^{\bullet}OH$ (k_{OH}, TBEP) 1.03×10^{10} M^{-1} s^{-1}) [29],. $^{\bullet}OH$ has been reported to be the major reactive species participating either in the photocatalytic degradation of structurally related flame retardants such as TCPP by nano-TiO_2 [23,26] or in chemical reactions taking place in environmental media such as atmosphere for TPhP (tri-phenyl-phosphate) [30].

3.2. *Identification of degradation products and photocatalytic mechanism*

The LIT-Orbitrap MS analysis was used to identify photocatalytic transformation products of TBEP and to propose pathways and mechanisms. Ten transformation products (TP1 to TP10) were detected during the photocatalytic degradation of TBEP by the catalysts. Their mass

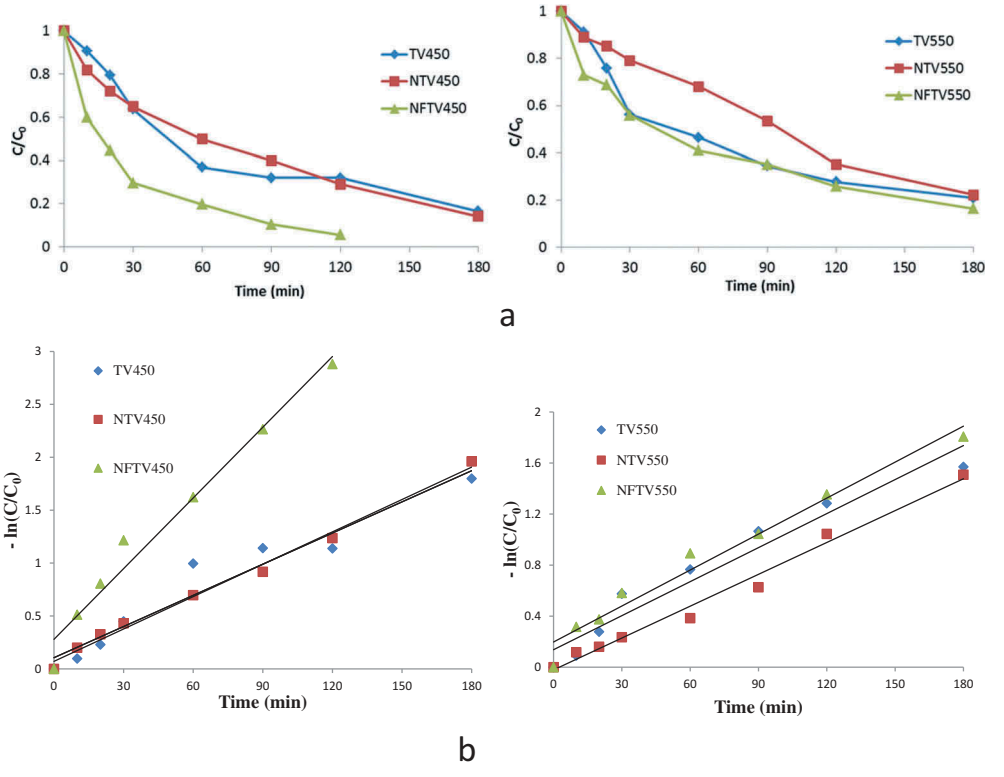

Figure 1. (a) Photocatalytic degradation kinetics of TBEP (0.5 mg L^{-1}) using different TiO_2/V_2O_5 photocatalysts. (b) Apparent first-order linear transform plots (-ln (C/Co) vs time) for TBEP (0.5 mg L^{-1}) photocatalytic degradation kinetics using different TiO_2/V_2O_5 photocatalysts.

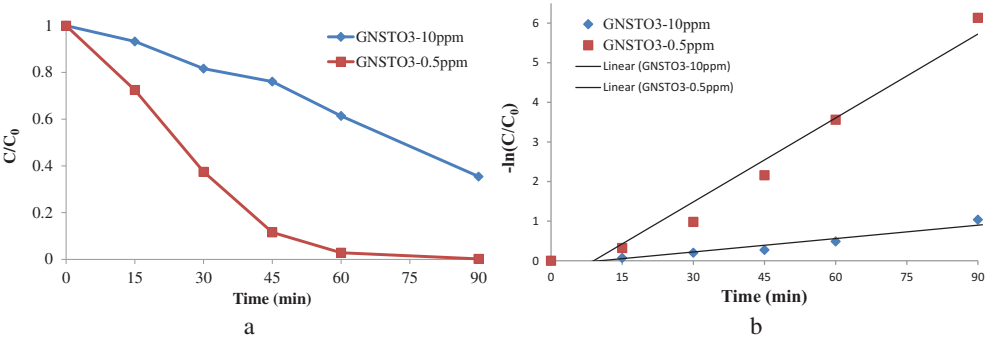

Figure 2. (a) Photocatalytic degradation kinetics of TBEP (10 and 0.5 mg L^{-1}) using N-doped $SrTiO_3$ catalyst. (b) Apparent first-order linear transform plots (-ln (C/Co) vs time) for TBEP (10 and 0.5 mg L^{-1}) photocatalytic degradation kinetics using N-doped $SrTiO_3$ catalyst.

spectra characteristics are presented in Table 2. Total ion (TIC) and extracted ion (EIC) chromatographic profiles of TPs are shown in Figure 3. Three TPs (TP2, TP3 and TP7) presented $[M + H]^+$ m/z ions of 415.2458 that differed 15.9953 units from the TBEP molecule ($[M + H]^+ = 399.2505$) and shorter retention times than TBEP (Figure 4, Table 2). Based on the

Table 1. Photocatalytic kinetics parameters (rate constants, half-life, R^2 for the first-order model) of TBEP using various photocatalysts.

	TBEP oxidation		
Catalyst	k (min^{-1})	$t_{1/2}$ (min)	R^2
TV 450	0.0098	70.7	0.9393
TV 550	0.0089	77.9	0.9441
NTV 450	0.0102	67.9	0.9920
NTV 550	0.0083	83.5	0.9853
NFTV 450	0.0233	29.7	0.9549
NFTV 550	0.0093	74.5	0.9549
G-NSTO3	0.071	9.8	0.9636

above characteristics, they were attributed to hydroxy-TBEP derivatives. TP4 with $[M + H]^+$ m/z ion of 413.2304 (Figure 4), that differed about 2 amu from the hydroxylated-TBEP, was assigned to carbonyl-derivatives. The presence of more than one isomeric derivatives was due to the non-selectivity of •OH radicals [12,16]. Consecutive •OH radicals attack led to the formation of three di-hydroxy-TBEP derivatives with $[M + H]^+$ = 431.2406 (Figure 4) that differed 31.9901 units from the TBEP molecule. The exact position of the •OH radical attack can be proposed from the analysis of the MS^2 spectra which is summarised in Table 2. For example, MS^2 ion with m/z = 331.1517, corresponding to the loss of – $C_6H_{12}O$ group, revealed the presence of one intact ether-chain. Furthermore, the MS^2 ion with m/z = 299.1612, corresponding to the loss of -$C_6H_{12}O_3$ group, reveals the existence of OH-groups in one of the ether-chains and especially in the butyl group taking into account the MS^2 ion at m/z = 343.1878 (loss of -$C_4H_8O_2$ group) and MS^3 ion m/z = 124.9997 ($C_2H_6PO_4^+$). In addition, for TP1, hydroxylation took place at the same ether chain due to the presence of characteristic MS^2 m/z ions at 355.1878 (loss of $C_3H_8O_2$) and 255.0992 (loss of $C_6H_{12}O$+$C_3H_8O_2$). Finally, TP 9 and 10 with $[M + H]^+$ m/z ions of 365.1698 and 299.1620 (Figure 4) respectively, presented characteristic losses of butyl (-C_4H_{10}) and butoxyethyl (-$C_6H_{12}O$) groups and were assigned to de-butyl-derivative and bi-(2-butoxyethyl) phosphate. Based on the time evolution of TPs (Figure 5) mono- and di-hydroxylation took place concurrently followed by dealkylation.

Figure 6 illustrates the proposed first stage transformation pathways of TBEP by •OH radical reaction. Pathway (I) involves hydrogen abstraction from the alkyl chains by •OH radical to produce initially a carbon-centred radical, which is followed by oxygen addition to generate the peroxyl radicals which then decomposed to hydroxylated and carbonylated derivatives via the bimolecular Russell mechanism [31]. The presence of heteroatoms (O) in the aliphatic chains of TBEP promoted the reactivity toward •OH [29,32]. Based on previous findings regarding hydroxyl radical attack on ether functions, hydrogen abstraction can take place both at α and β positions of the ether function but with a greater selectivity (about 78%) in α position [33].

Pathway B involves •OH radical addition to the phosphorus atom to yield an oxygen-centred phosphoryl radical, which is followed by the elimination of the butoxyethyl chain from the phosphate moiety. Hydrogen abstraction and addition-elimination mechanisms are also proposed as primary mechanisms for the photocatalytic oxidation of other organophosphate compounds such as dimethyl methylphosphonate and TCEP

Table 2. LC–MS summary data (Retention time, R_t; *m/z* ions $[M + H]^+$; molecular formulae; relative error Δ(ppm) and ring-double-bond equivalents, RDBE) for TBEP and DPs.

TP	R_t	$[M+H]^+$	Structure	Assignment	Δ(ppm)	RDBE	MS^2	Structure	Δ (ppm)	RDBE
-	15.51	399.2505	$C_{18}H_{40}O_7P$	TBEP	-0.242	-0.5	299.1622	$C_{12}H_{28}O_6P$	0.365	-0.5
		421.2314	$C_{18}H_{39}O_7PNa$	TBEP+Na	-3.635	-0.5	199.0733	$C_6H_{16}O_5P$	0.313	-0.5
		299.1621	$C_{12}H_{28}O_6P$	BDEP	0.931	-0.5				
TP1	14.12	431.2406	$C18H_{40}O_9P$	TBEP+2OH	0.358	-0.5	355.1878	$C_{15}H_{32}O_7P$	-0.176	0.5
							299.1612	$C_{12}H_{28}O_6P$	-0.612	-0.5
							255.0992	$C_9H_{20}O_6P$	0.039	0.5
							225.0885	$C_8H_{18}O_5P$	0.147	0.5
							155.0101	$C_3H_8O_5P$	0.266	0.5
TP2	14.24	415.2458	$C_{18}H_{40}O_8P$	TBEP+OH	0.696	-0.5				
		437.2275	$C_{18}H_{39}O_8PNa$	TBEP+OH+Na	-3.307	-0.5				
TP3	13.99	415.2458	$C_{18}H_{40}O_8P$	TBEP+OH	0.407	-0.5				
TP4	13.75	413.2304	$C_{18}H_{38}O_8P$	TBEP=O	1.353	0.5				
TP5	13.71	431.2410	$C_{18}H_{40}O_9P$	TBEP+2OH	1.285	-0.5	343.1878	$C_{14}H_{32}O_7P$	-0.176	0.5
							331.1517	$C_{12}H_{28}O_8P$	0.069	-0.5
							299.1619	$C_{12}H_{28}O_6P$	0.068	-0.5
							269.1148	$C_{10}H_{22}O_6P$	0.071	0.5
							243.0993	$C_8H_{20}O_6P$	0.059	-0.5
							225.0885	$C_8H_{18}O_5P$	-0.147	0.5
							199.0730	$C_6H_{16}O_5P$	0.053	-0.5
							169.0260	$C_4H_{10}O_5P$	-0.036	0.5
TP6	13.58	431.2409	$C_{18}H_{40}O_9P$	TBEP+2OH	1.077	-0.5	331.1516	$C_{12}H_{28}O_8P$	-0.081	-0.5
							299.1615	$C_{12}H_{28}O_6P$	-0.272	-0.5
							243.0992	$C_8H_{20}O_6P$	0.009	-0.5
							225.0884	$C_8H_{18}O_5P$	-0.247	0.5
							199.0729	$C_6H_{16}O_5P$	-0.067	-0.5
TP7	13.63	415.2460	$C_{18}H_{40}O_8P$	TBEP+OH	0.985	-0.5				
TP8	13.46	413.2303	$C_{18}H_{38}O_8P$	TBEP=O	-2.561	0.5	343.1883	$C_{14}H_{32}O_7P$	0.304	-0.5
							313.1412	$C_{12}H_{26}O_7P$	0.104	0.5
							299.1677	$C_{12}H_{28}O_6P$	-0.122	-0.5
							243.0993	$C_8H_{20}O_6P$	0.089	-0.5
TP9	12.77	365.1698	$C_{16}H_{30}O_7P$ Na	TBEP-C_4H_{10}	-2.596	2.5	299.1617	$C_{12}H_{28}O_6P$	-0.062	-0.5
		343.1880	$C_{14}H_{32}O_7P$		0.011	-0.5	243.0992	$C_8H_{20}O_6P$	-0.021	-0.5
							225.0888	$C_8H_{18}O_5P$	0.153	0.5
							199.0730	$C_6H_{16}O_5P$	0.053	-0.5
							143.0102	$C_2H_8O_5P$	-0.146	-0.5
							124.9995	C_2H6O_4P	-0.272	05
TP10	11.75	299.1621	$C_{12}H_{28}O_6P$	BDEP	0.831	-0.5	199.0728	$C_6H_{16}O_5P$	-0.177	-0.5
		321.1438	$C_{12}H_{27}O_6PNa$	BDEP+Na	0.261	-0.5	143.0101	$C_2H_8O_5P$	-0.286	-0.5

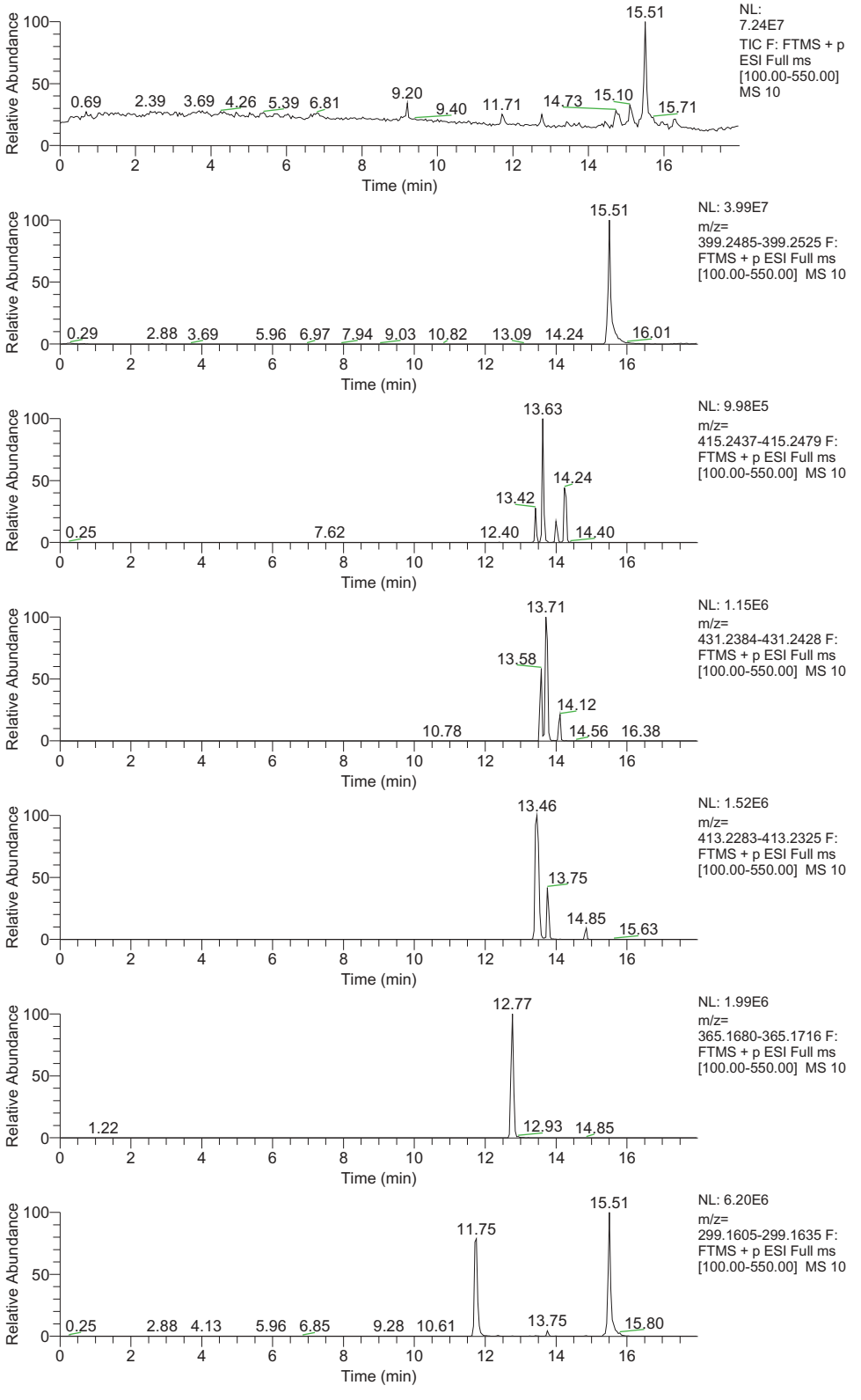

Figure 3. Total ion and extracted ion chromatograms of TBEP and its photocatalytic degradation.

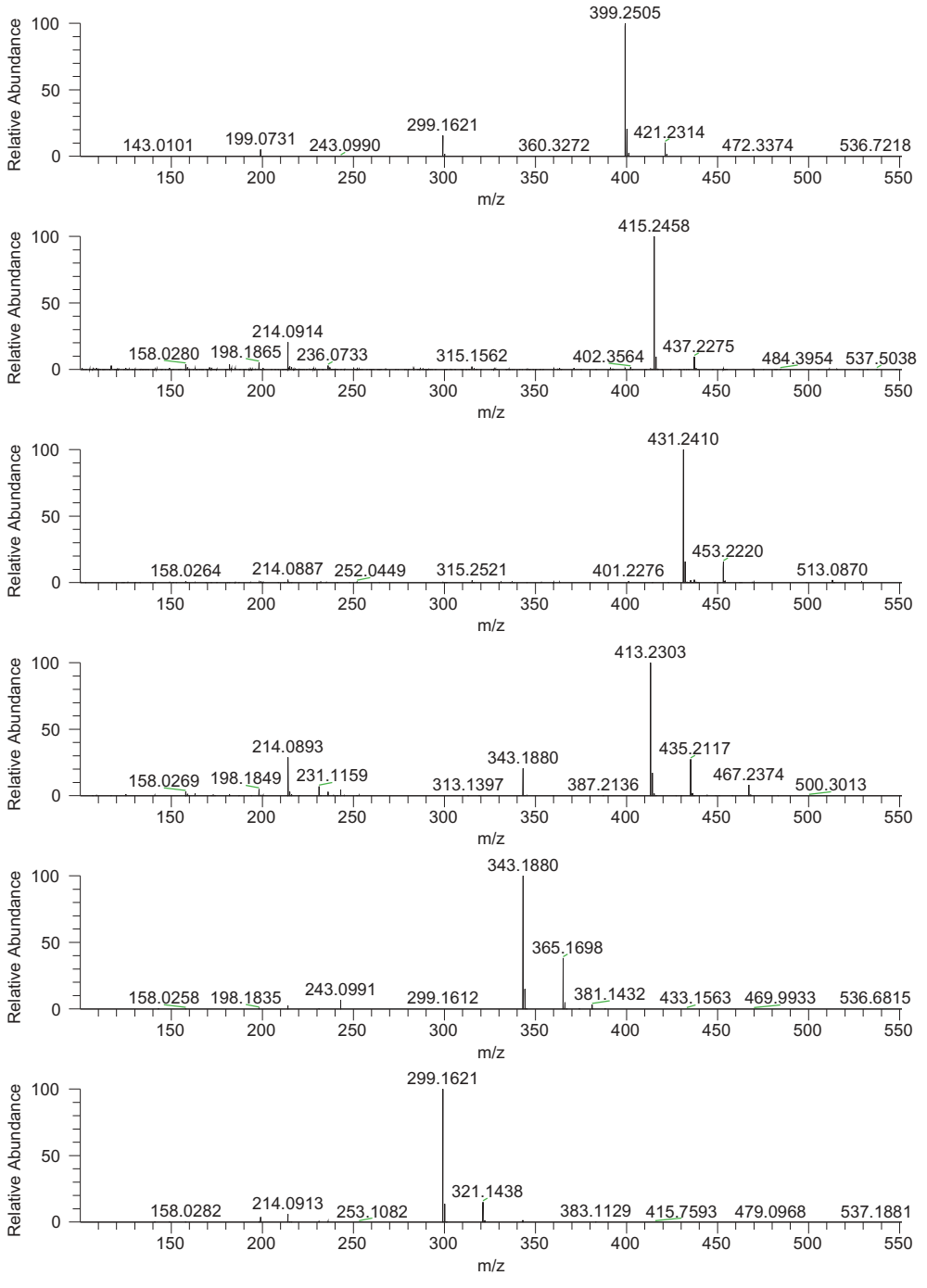

Figure 4. LC-ESI-LIT-Orbitrap MS spectra of TBEP and transformation products.

via hydroxyl radical attack [34,35]. Based on the identified TPs and the proposed mechanisms, Figure 7 summarises the probable photocatalytic transformation pathways of TBEP.

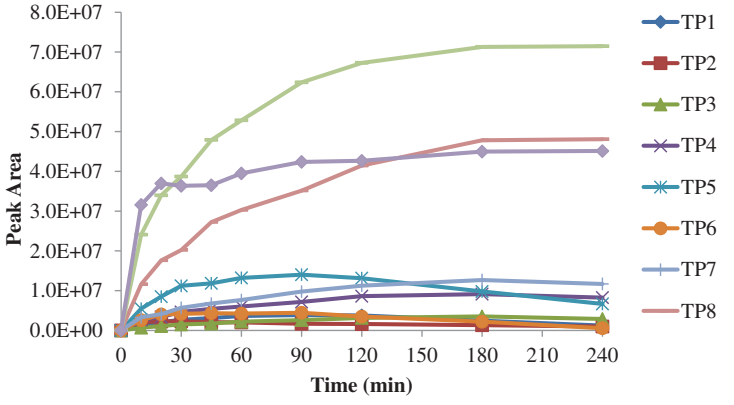

Figure 5. Time-evolution of photocatalytic degradation products of TBEP (10 mgL^{-1}) in the presence of visible-light catalysts.

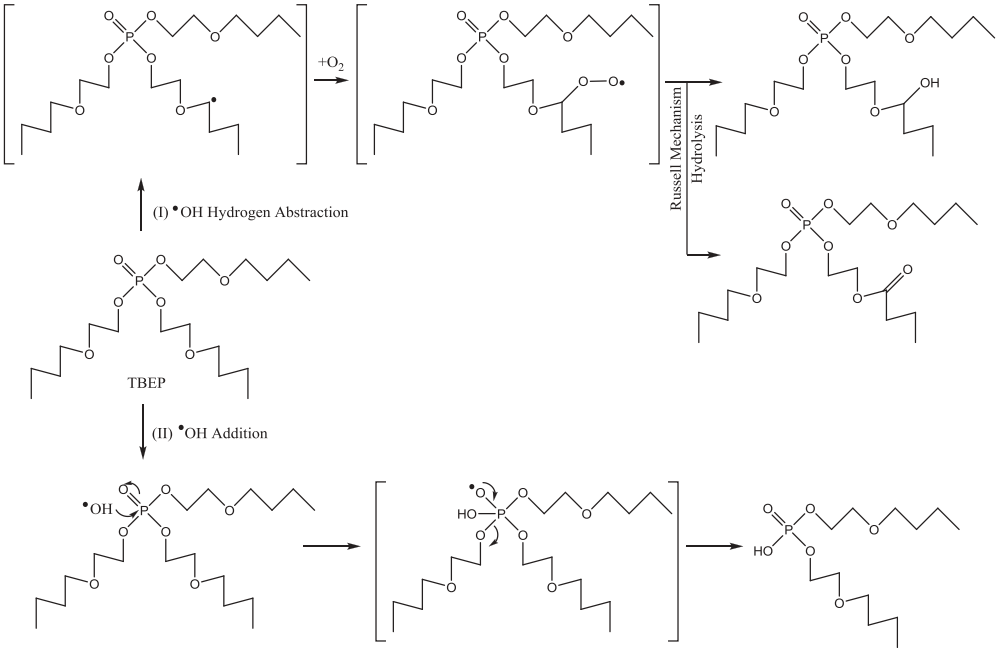

Figure 6. Proposed mechanisms for TBEP degradation by photocatalytically generated •OH radicals.

4. Conclusions

The kinetics and mechanisms of TBEP flame retardant photocatalytic degradation were studied using TiO_2/V_2O_5 and N-doped-$SrTiO_3$ as catalysts. N-doped-$SrTiO_3$ was found to be the most efficient catalyst; the activity of all catalysts studied was found to depend on their ability to generate •OH radicals. The transformation products have been successfully identified using high-resolution liquid

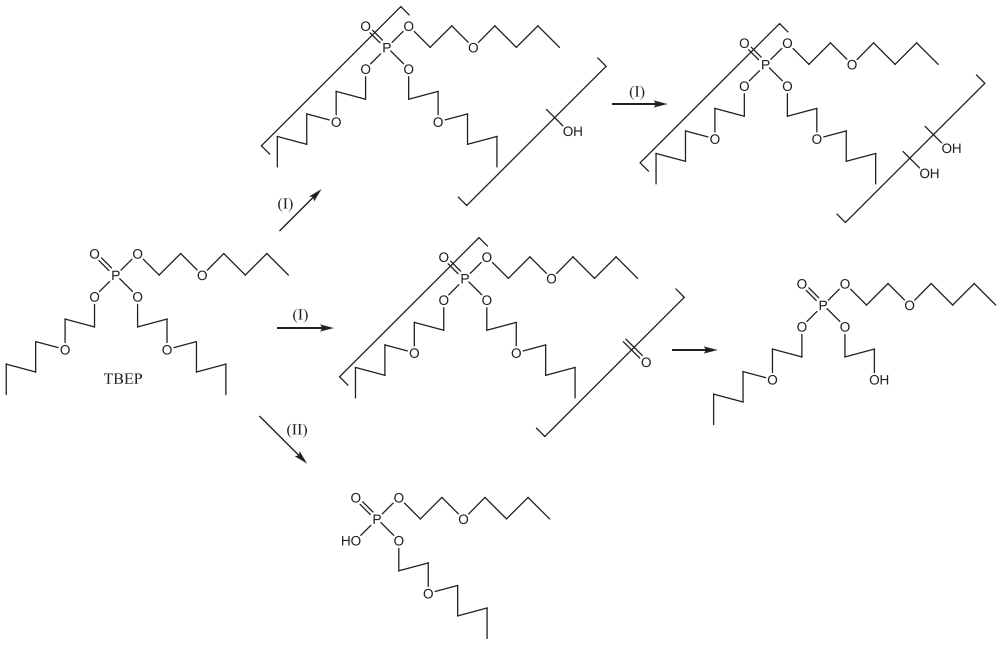

Figure 7. Tentative photocatalytic degradation pathways of TBEP in the presence of visible-light catalysts.

chromatography – mass spectrometry. Degradation pathways involve hydroxyl radicals and proceed via multiple hydroxylation and oxidation steps progressively leading to dealkylation of TBEP.

Acknowledgments

The authors would like to thank the Unit of Environmental, Organic and Biochemical high-resolution analysis-orbitrap-LC–MS analysis of the University of Ioannina for providing access to the facilities.

Disclosure statement

No potential conflict of interest was reported by the authors.

References

[1] I.K. Konstantinou and T.A. Albanis, Appl. Catal. B: Environ. **49**, 1 (2004). doi:10.1016/j.apcatb.2003.11.010.
[2] M. Pelaez, N.T. Nolan, S.C. Pillai, M.K. Seery, P. Falaras, A.G. Kontos, P.S.M. Dunlop, J.W. J. Hamilton, J.W. Byrne, K. O'Shea, M.H. Entezari and D.D. Dionysiou, Appl. Catal. B: Environ. **125**, 331 (2012). doi:10.1016/j.apcatb.2012.05.036.
[3] J. Cristale, A. Garcia Vazquez, C. Barata and S. Lacorte, Environ. Int. **59**, 232 (2013). doi:10.1016/j.envint.2013.06.011.
[4] I. Watanabe and S.-I. Sakai, Environ. Int. **29**, 665 (2003). doi:10.1016/S0160-4120(02)00167-8.

[5] F. Bettazzi, T. Martellini, W.L. Shelver, A. Cincinelli, E. Lanciotti and I. Palchetti, Electroanalysis **28**, 1817 (2016). doi:10.1002/elan.201600127.
[6] V. Linares, M. Bellés and J.L. Domingo, Arch. Toxicol. **89**, 335 (2015). doi:10.1007/s00204-015-1457-1.
[7] L.S. Birnbaum and D.F. Staskal, Environ. Health Perspect. **112**, 9 (2004). doi:10.1289/ehp.6559.
[8] M. Iqbal, J.H. Syed, A. Katsoyiannis, R. Naseem Malik, A.A. Farooqi, A. Butt, J. Lib, G. Zhang, A. Cincinelli and K.C. Jones, Environ. Res. **152**, 26 (2017). doi:10.1016/j.envres.2016.09.024.
[9] Y.X. Ou, Chem. Ind. Eng. Prog. **30**, 210 (2011). (In Chinese).
[10] Å. Bergman, A. Ryden, R.J. Law, J. de Boer, A. Covaci, M. Alaee, L. Birnbaum, M. Petreas, M. Rose, S. Sakai, N. Van Den Eede and I. van der Veen, Environ. Int. **49**, 57 (2012). doi:10.1016/j.envint.2012.08.003.
[11] I. van der Veen and J. de Boer, Chemosphere **88**, 1119 (2012). doi:10.1016/j.chemosphere.2012.03.067.
[12] G.L. Wei, D.Q. Li, M.N. Zhuo, Y.S. Liao, Z.Y. Xie, T.L. Guo, J.J. Li, S.Y. Zhang and Z.Q. Liang, Environ. Pollut. **196**, 29 (2015). doi:10.1016/j.envpol.2014.09.012.
[13] J.A. Andresen, A. Grundmann and K. Bester, Sci. Total Environ. **332**, 155 (2004). doi:10.1016/j.scitotenv.2004.04.021.
[14] J. Li, N. Yu, B. Zhang, L. Jin, M. Li, M. Hua, X. Zhang, S. Wei and H. Yu, Water Res. **54**, 53 (2014). doi:10.1016/j.watres.2014.01.031.
[15] A. Marklund, B. Andersson and P. Haglund, Environ. Sci. Technol. **39**, 7423 (2005). doi:10.1021/es051013l.
[16] R. Loos, R. Carvalho, D.C. Antonio, S. Comero, G. Locoro, S. Tavazzi, B. Paracchini, M. Ghiani, T. Lettieri, L. Blaha, B. Jarosova, S. Voorspoels, K. Servaes, P. Haglund, J. Fick, R.H. Lindberg, D. Schwesig and B.M. Gawlik, Water Res. **47**, 6475 (2013). doi:10.1016/j.watres.2013.08.024.
[17] E. Martínez-Carballo, C. González-Barreiro, A. Sitka, S. Scharf and O. Gans, Sci. Total Environ. **388**, 290 (2007). doi:10.1016/j.scitotenv.2007.08.005.
[18] K.L. Chow, Y.B. Man, J.S. Zheng, Y. Liang, N.F.Y. Tam and M.H. Wong, J Environ. Sci. (China) **24**, 1670 (2012). doi:10.1016/S1001-0742(11)60992-3.
[19] Y. Guo, X. Lou, D. Xiao, L. Xu, Z. Wang and J. Liu, J Hazard. Mater. **241–242**, 301 (2012). doi:10.1016/j.jhazmat.2012.09.044.
[20] A. Huang, N. Wang, M. Lei, L. Zhu, Y. Zhang, Z. Lin, D. Yin and H. Tang, Environ. Sci. Technol. **47** (1), 518 (2013). doi:10.1021/es302935e.
[21] M. Cao, P. Wang, Y. Ao, C. Wang, J. Hou and J. Qian, Chem. Eng. J. **264**, 113 (2015). doi:10.1016/j.cej.2014.10.011.
[22] X. Peng, W. Li, J. Chen and X. Jia, Desalination Water Treat. **65**, 451 (2017). doi:10.5004/dwt.2017.20232.
[23] M. Antonopoulou, P. Karagianni and I.K. Konstantinou, Appl. Catal. B: Environ. **192**, 152 (2016). doi:10.1016/j.apcatb.2016.03.039.
[24] J. Ye, J. Liu, C. Li, P. Zhou, S. Wu and H. Ou, Water Res. **124**, 29 (2017). doi:10.1016/j.watres.2017.07.034.
[25] M. Antonopoulou, A. Giannakas, F. Bairamis, M. Papadaki and I. Konstantinou, Chem. Eng. J. **318**, 231 (2017). doi:10.1016/j.cej.2016.06.124.
[26] T. Tang, G. Lu, W. Wang, R. Wang, K. Huang, Z. Qiu, X. Tao and Z. Dang, Chemosphere **206**, 26 (2018). doi:10.1016/j.chemosphere.2018.04.161.
[27] A. Giannakas, F. Bairamis, I. Papakostas, T. Zerva and I. Konstantinou, J. Ind. Eng. Chem. **318**, 231 (2018). doi:10.1016/j.jiec.2018.05.008.
[28] P.-S. Konstas, I. Konstantinou, D. Petrakis and T. Albanis, Catalysts **8**, 258 (2018). doi:10.3390/catal8110528.
[29] M.J. Watts and K.G. Linden, Environ. Sci. Technol. **43**, 2937 (2009). doi:10.1021/es8031659.
[30] Q. Yu, H.-B. Xie and J. Chen, Sci. Total. Environ. **571**, 1105 (2016). doi:10.1016/j.scitotenv.2016.07.105.
[31] X. Pang, C. Chen, H. Ji, Y. Che, W. Ma and J. Zhao, Molecules **19**, 16291 (2014). doi:10.3390/molecules191016291.

[32] X. Yuan, S. Lacorte, J. Cristale, R.F. Dantas, C. Sans, S. Esplugas and Z. Qiang, Sep. Purif. Technol. **156**, 1028 (2015). doi:10.1016/j.seppur.2015.09.052.
[33] M.N. Schuchmann, C. von Sonntag. and Z. Naturforsch, **42b**, 495 (1987).
[34] A. Aguila, K.E. O'Shea, T. Tobien and K.D. Asmus, J. Phys. Chem. A **105**, 7834 (2001). doi:10.1021/jp002367w.
[35] L. Wu, B. Chládková, O.J. Lechtenfeld, S. Lian, J. Schindelka, H. Herrmann and H.H. Richnow, Sci. Total Environ. **615**, 20 (2018). doi:10.1016/j.scitotenv.2017.09.233.